

# 1 MeLSI: Metric Learning for Statistical Inference in 2 Microbiome Community Composition Analysis

3 **Nathan Bresette<sup>1,2</sup>, Aaron C. Ericsson<sup>3,4</sup>, Carter Woods<sup>1</sup>, Ai-Ling Lin<sup>1,2,5,6,\*</sup>**

4 AUTHOR AFFILIATIONS See affiliation list .

- 5 • Corresponding author: Ai-Ling Lin, ai-ling.lin@health.missouri.edu

## 6 ABSTRACT

7 Microbiome beta diversity analysis relies on distance-based methods including  
8 PERMANOVA combined with fixed ecological distance metrics (Bray-Curtis, Euclidean,  
9 Jaccard, and UniFrac), which treat all microbial taxa uniformly regardless of their biological  
10 relevance to community differences. This “one-size-fits-all” approach may miss subtle but  
11 biologically meaningful patterns in complex microbiome data. We present MeLSI (Metric  
12 Learning for Statistical Inference), a novel machine learning framework that learns data-  
13 adaptive distance metrics optimized for detecting community composition differences in  
14 multivariate microbiome analyses. MeLSI employs an ensemble of weak learners using  
15 bootstrap sampling, feature subsampling, and gradient-based optimization to learn  
16 optimal feature weights, combined with rigorous permutation testing for statistical  
17 inference. The learned metrics can be used with PERMANOVA for hypothesis testing and  
18 with Principal Coordinates Analysis (PCoA) for ordination visualization. Comprehensive  
19 validation on synthetic benchmarks and real datasets shows that MeLSI maintains proper  
20 Type I error control while delivering competitive or superior F-statistics when signal  
21 structure aligns with CLR-based weighting and, crucially, supplies interpretable feature-  
22 weight profiles that clarify which taxa drive group separation. On the Atlas1006 dataset,  
23 MeLSI achieved stronger effect sizes than the best traditional methods, and even when  
24 performance was comparable, the learned feature weights provided biological insight that  
25 fixed metrics cannot supply. MeLSI therefore offers a statistically rigorous tool that  
26 augments beta diversity analysis with transparent, data-driven interpretability.

## 27 IMPORTANCE

28 Understanding which microbes differ between groups of interest could reveal therapeutic  
29 targets and diagnostic biomarkers. However, current analysis methods treat all microbes  
30 equally (similar to using the same ruler to measure everything, regardless of what matters  
31 most). This means subtle but clinically important differences may go undetected,  
32 especially when only a few key species drive disease while hundreds of “bystander”  
33 species add noise. MeLSI solves this by learning which microbes matter most for each  
34 specific comparison. In comparing male and female gut microbiomes, MeLSI identified  
35 specific bacterial families driving the differences, providing actionable biological insights  
36 that standard methods miss. This capability is particularly crucial for detecting early

37 disease biomarkers, where differences are subtle and masked by biological variability. By  
38 telling researchers not just whether groups differ, but which specific microbes drive those  
39 differences, MeLSI accelerates the path from microbiome data to testable biological  
40 hypotheses and clinical applications.

41 **Keywords:** microbiome analysis, metric learning, beta diversity, community composition,  
42 PERMANOVA, distance metrics, permutation testing

## 43 INTRODUCTION

### 44 The microbiome and human health

45 The human microbiome, the complex community of microorganisms inhabiting our bodies,  
46 plays fundamental roles in health and disease (1, 2). Recent advances in high-throughput  
47 sequencing technologies have enabled comprehensive profiling of microbial communities,  
48 revealing associations between microbiome composition and diverse conditions including  
49 inflammatory bowel disease, obesity, diabetes, and neurological disorders (3, 4). A central  
50 question in microbiome research is comparing overall microbial community composition  
51 between groups of interest, typically assessed through beta diversity analysis, which  
52 studies compositional differences between samples.

### 53 Current approaches and their limitations

54 Microbiome beta diversity analysis predominantly relies on distance-based multivariate  
55 methods including PERMANOVA (Permutational Multivariate Analysis of Variance)  
56 combined with fixed ecological distance metrics (5, 6). Commonly used metrics include  
57 Bray-Curtis dissimilarity, Euclidean distance, Jaccard index, and phylogenetically-  
58 informed metrics including UniFrac (7). These approaches have proven valuable for  
59 hypothesis testing about community differences and visualization through ordination  
60 methods such as Principal Coordinates Analysis (PCoA) (8).

61 However, fixed distance metrics suffer from a fundamental limitation. They apply the same  
62 mathematical formula to all datasets, treating all microbial taxa with equal importance  
63 regardless of their biological relevance to the specific research question (9). For instance,  
64 Bray-Curtis dissimilarity equally weights all taxa based on their relative abundances, while  
65 Euclidean distance treats all features identically. This “one-size-fits-all” approach may fail  
66 to capture subtle but biologically meaningful differences when only a subset of taxa drive  
67 group separation (10).

68 Furthermore, microbiome data presents unique analytical challenges including high  
69 dimensionality (often hundreds to thousands of taxa), compositionality (relative  
70 abundances sum to a constant), sparsity (many zero counts), and heterogeneous  
71 biological signal across features (11). Fixed metrics cannot adapt to these complexities in  
72 a data-driven manner.

73 **The need for statistical rigor**

74 A critical requirement for any beta diversity method is proper statistical inference with  
75 controlled Type I error rates (false positive rates). While machine learning approaches  
76 often prioritize predictive accuracy, hypothesis testing for community composition  
77 differences requires rigorous F-statistic and p-value calculation under the null hypothesis  
78 of no group differences (12). Permutation testing provides a non-parametric framework for  
79 valid inference that makes minimal distributional assumptions (13), making it particularly  
80 suitable for complex microbiome data and distance-based analyses such as PERMANOVA.

81 **Metric learning: an emerging paradigm**

82 Metric learning, a branch of machine learning, offers a principled approach to address  
83 these limitations (14, 15). Rather than using fixed distance formulas, metric learning  
84 algorithms learn optimal distance metrics from data by identifying which features  
85 contribute most to separating groups of interest. In the context of supervised learning,  
86 metric learning algorithms optimize distance functions to maximize between-group  
87 distances while minimizing within-group distances (16, 17).

88 We formalize metric learning as follows: Let  $\mathbf{X} \in \mathbb{R}^{n \times p}$  denote a feature abundance matrix  
89 with  $n$  samples and  $p$  taxa, and let  $\mathbf{y} = (y_1, \dots, y_n)$  denote group labels. A distance metric is  
90 parameterized by a positive semi-definite matrix  $\mathbf{M} \in \mathbb{R}^{p \times p}$ , where the Mahalanobis  
91 distance between samples  $i$  and  $j$  is  $d_M(\mathbf{x}_i, \mathbf{x}_j) = \sqrt{(\mathbf{x}_i - \mathbf{x}_j)^T \mathbf{M} (\mathbf{x}_i - \mathbf{x}_j)}$ . For diagonal  $\mathbf{M}$ ,  
92 this reduces to weighted Euclidean distance with feature-specific weights  $M_{jj}$  representing  
93 the importance of feature  $j$ .

94 Mahalanobis distance learning (18) learns a positive semi-definite matrix  $\mathbf{M}$  that defines  
95 distances as  $d(\mathbf{x}_i, \mathbf{x}_j) = \sqrt{(\mathbf{x}_i - \mathbf{x}_j)^T \mathbf{M} (\mathbf{x}_i - \mathbf{x}_j)}$ . When  $\mathbf{M}$  is diagonal, this reduces to  
96 learning feature-specific weights, providing interpretable importance scores (17).

97 Despite its promise, metric learning has seen limited application in microbiome beta  
98 diversity analysis. Previous work has explored metric learning for clinical prediction tasks  
99 (19), but not specifically for statistical inference in community composition analysis where  
100 rigorous Type I error control is essential.

101 **Study objectives**

102 We developed MeLSI (Metric Learning for Statistical Inference) to bridge the gap between  
103 adaptive machine learning approaches and rigorous statistical inference for microbiome  
104 beta diversity and community composition analysis. Our specific objectives were to (1)  
105 design an ensemble metric learning framework that learns data-adaptive distance metrics  
106 for PERMANOVA and ordination while preventing overfitting, (2) integrate metric learning  
107 with permutation testing to ensure valid statistical inference, (3) comprehensively validate  
108 Type I error control, statistical power, scalability, parameter sensitivity, and computational  
109 efficiency, (4) demonstrate practical utility on real microbiome datasets, and (5) provide

110 interpretable feature importance scores to identify biologically relevant taxa driving  
111 community separation.

112 This paper presents the MeLSI framework, comprehensive validation results, and  
113 discussion of its implications for microbiome beta diversity research.

## 114 MATERIALS AND METHODS

### 115 Overview of the MeLSI framework

116 MeLSI integrates metric learning with permutation-based statistical inference through two  
117 main phases:

#### 118 Phase 1: Metric Learning

- 119 1. Apply conservative pre-filtering to focus on high-variance features
- 120 2. For each of B weak learners:
  - 121 o Bootstrap sample the data
  - 122 o Subsample features
  - 123 o Optimize metric matrix  $\mathbf{M}$  via gradient descent
- 124 3. Combine weak learners via performance-weighted ensemble averaging
- 125 4. Compute robust distance matrix using eigenvalue decomposition

#### 126 Phase 2: Statistical Inference

- 127 5. Calculate observed F-statistic using the learned metric
- 128 6. Generate null distribution via permutation testing (relearn metric on each  
129 permutation)
- 130 7. Compute permutation-based p-value

131 Each component addresses specific challenges in microbiome data analysis while  
132 maintaining statistical validity. The following sections formalize the mathematical  
133 framework and detail each algorithmic component, organized by phase.

#### 134 Phase 1: Metric Learning

##### 135 *Problem formulation*

136 Let  $\mathbf{X} \in \mathbb{R}^{n \times p}$  denote a feature abundance matrix with  $n$  samples and  $p$  taxa (features), and  
137 let  $\mathbf{y} = (y_1, \dots, y_n)$  denote group labels. Our goal is to learn a distance metric optimized for  
138 separating groups defined by  $\mathbf{y}$  while ensuring valid statistical inference.

139 We parameterize the distance metric using a diagonal positive semi-definite matrix  $\mathbf{M} \in$   
140  $\mathbb{R}^{p \times p}$ , where  $M_{jj}$  represents the weight (importance) of feature  $j$ . The learned Mahalanobis  
141 distance between samples  $i$  and  $k$  is:

$$142 d_M(\mathbf{x}_i, \mathbf{x}_k) = \sqrt{(\mathbf{x}_i - \mathbf{x}_k)^T \mathbf{M} (\mathbf{x}_i - \mathbf{x}_k)}$$

143 For diagonal  $\mathbf{M}$ , this simplifies to a weighted Euclidean distance:

144

145 
$$d_M(\mathbf{x}_i, \mathbf{x}_k) = \sqrt{\sum_j M_{jj} (x_{ij} - x_{kj})^2}$$

146 *Conservative pre-filtering*

147 To improve computational efficiency and reduce noise, MeLSI applies conservative  
148 variance-based pre-filtering. For pairwise comparisons, we calculate a feature importance  
149 score combining mean differences and variance:

150

151 
$$I_j = \frac{|\mu_{1j} - \mu_{2j}|}{\sqrt{\sigma_{1j}^2 + \sigma_{2j}^2}}$$

152 where  $\mu_{1j}$  and  $\mu_{2j}$  are the mean abundances of feature  $j$  in groups 1 and 2, and  $\sigma_{1j}^2$  and  $\sigma_{2j}^2$   
153 are their variances. We retain the top 70% of features by this importance score,  
154 maintaining high statistical power while reducing dimensionality.

155 For multi-group comparisons (3 or more groups), we use ANOVA F-statistics to rank  
156 features and apply the same 70% retention threshold. These statistics serve as ranking  
157 heuristics to order features by between-group differences relative to within-group variation;  
158 no distributional assumptions are required because all statistical inference uses  
159 permutation testing. Critically, this pre-filtering is applied consistently to both observed  
160 and permuted data during null distribution generation to avoid bias.

161 *Ensemble learning with weak learners*

162 MeLSI constructs an ensemble of  $B$  weak learners (default  $B = 30$ ) to improve robustness  
163 and prevent overfitting. For each weak learner  $b$ :

- 164 1. **Bootstrap sampling:** Draw  $n$  samples with replacement from the original data to  
165 create a bootstrap dataset  $(\mathbf{X}_b, \mathbf{y}_b)$
- 166 2. **Feature subsampling:** Randomly select  $m = \lfloor p \times m_{frac} \rfloor$  features (default  $m_{frac} =$   
167 0.8) without replacement
- 168 3. **Metric optimization:** Learn  $\mathbf{M}_b$  on the bootstrapped, subsampled data

169 The combination of bootstrap sampling (sample-level randomness) and feature  
170 subsampling (feature-level randomness) ensures diversity among weak learners, reducing  
171 overfitting risk (20).

172    *Optimization objective*

173    For each weak learner, we optimize  $\mathbf{M}$  to maximize between-group distances while  
174    minimizing within-group distances. For a two-group comparison (groups  $G_1$  and  $G_2$ ), we  
175    maximize the objective:

$$176 \quad F(\mathbf{M}) = \frac{1}{|G_1||G_2|} \sum_{i \in G_1} \sum_{k \in G_2} d_M(\mathbf{x}_i, \mathbf{x}_k)^2 - \frac{1}{2|G_1|^2} \sum_{i,j \in G_1} d_M(\mathbf{x}_i, \mathbf{x}_j)^2 - \frac{1}{2|G_2|^2} \sum_{i,j \in G_2} d_M(\mathbf{x}_i, \mathbf{x}_j)^2$$

177    This objective encourages large between-group distances and small within-group  
178    distances, analogous to maximizing the F-ratio in ANOVA. This formulation is inspired by  
179    standard metric learning objectives that maximize between-class to within-class distance  
180    ratios (17, 16), adapted here for direct compatibility with PERMANOVA's F-statistic  
181    framework.

182    *Gradient-based optimization*

183    Each weak learner optimizes its metric matrix  $\mathbf{M}$  using stochastic gradient descent,  
184    sampling within-group and between-group pairs to compute gradients that maximize  
185    between-group distances while minimizing within-group distances. We use an adaptive  
186    learning rate  $\eta_t = \eta_0 / (1 + 0.1t)$  (default  $\eta_0 = 0.1$ ) and constrain  $M_{jj} \geq 0.01$  to ensure  
187    positive definiteness. Early stopping monitors F-statistics every 20 iterations, terminating if  
188    performance stagnates (no improvement for 5 consecutive checks) to prevent overfitting.

189    *Ensemble averaging with performance weighting*

190    After training all weak learners, we combine them into a final ensemble metric  $\mathbf{M}_{ensemble}$   
191    using performance-weighted averaging:

$$192 \quad \mathbf{M}_{ensemble} = \sum_b w_b \mathbf{M}_b$$

193    where weights are normalized F-statistics:

$$194 \quad w_b = \frac{F_b}{\sum_{b'} F_{b'}}$$

195    and  $F_b$  is the PERMANOVA F-statistic achieved by weak learner  $b$  on its bootstrap sample.  
196    This weighting scheme emphasizes better-performing learners while maintaining diversity.

197    *Robust distance calculation*

198    To ensure numerical stability, we compute the learned Mahalanobis distance using  
199    eigenvalue decomposition:

- 200    1. Compute eigendecomposition:  $\mathbf{M}_{ensemble} = \mathbf{V}\Lambda\mathbf{V}^T$  where  $\mathbf{V}$  is the matrix of  
201    eigenvectors and  $\Lambda$  is the diagonal matrix of eigenvalues
- 202    2. Enforce positive eigenvalues:  $\max(\Lambda_{ii}, 10^{-6}) \rightarrow \Lambda_{ii}$

- 203        3. Compute  $\mathbf{M}^{-1/2} = \mathbf{V}\Lambda^{-1/2}\mathbf{V}^T$   
 204        4. Transform data:  $\mathbf{Y} = \mathbf{X}\mathbf{M}^{-1/2}$   
 205        5. Calculate Euclidean distances in transformed space:  $d_M = \|\mathbf{y}_i - \mathbf{y}_k\|_2$

206        This approach is more numerically stable than direct matrix inversion, particularly for high-  
 207        dimensional data.

## 208        Phase 2: Statistical Inference

209        Phase 2 focuses on statistical inference using the learned metric from Phase 1. We  
 210        compute p-values through permutation testing to ensure valid statistical inference.

### 211        Statistical inference via permutation testing

#### 212        *Test statistic*

213        We use the PERMANOVA F-statistic as our test statistic (5):

$$214 \quad F_{obs} = \frac{SS_{between}/(k - 1)}{SS_{within}/(n - k)}$$

215        where  $SS_{between}$  is the between-group sum of squares,  $SS_{within}$  is the within-group sum of  
 216        squares,  $k$  is the number of groups, and  $n$  is the total number of samples. This statistic  
 217        measures how well the learned metric separates groups relative to within-group variation.

#### 218        *Null distribution generation*

219        To compute valid p-values, we generate a null distribution under the hypothesis of no  
 220        group differences:

- 221        1. Permute group labels: random permutation of  $\mathbf{y} \rightarrow \mathbf{y}_{perm}$
- 222        2. Apply identical pre-filtering to permuted data
- 223        3. Learn metric  $\mathbf{M}_{perm}$  on  $(\mathbf{X}_{filtered}, \mathbf{y}_{perm})$  using the full MeLSI algorithm (repeating  
             Phase 1: pre-filtering, ensemble construction, and metric optimization)
- 224        4. Calculate  $F_{perm}$  on  $(\mathbf{X}_{filtered}, \mathbf{y}_{perm})$  with  $\mathbf{M}_{perm}$
- 225        5. Repeat steps 1-4 for  $n_{perms}$  permutations (default  $n_{perms} = 200$ )

227        This approach ensures that the null distribution accurately reflects the variability  
 228        introduced by the metric learning procedure itself, avoiding anticonservative (inflated Type  
 229        I error) inference.

#### 230        *P-value calculation*

231        The permutation-based p-value is computed as:

$$232 \quad p = \frac{\sum \mathbb{I}(F_{perm} \geq F_{obs}) + 1}{n_{perms} + 1}$$

233 where  $\mathbb{I}$  is the indicator function. The “+1” terms provide a small-sample correction  
234 ensuring  $p \geq 1/(n_{perms} + 1)$  (21).

## 235 Validation experiments

236 We conducted comprehensive validation experiments to assess:

237 . Type I error control and statistical power: Performance on null data (no true group  
238 differences) and ability to detect true effects of varying magnitude across synthetic  
239 datasets (Sections 3.1-3.2) 2. Scalability: Performance across varying sample sizes and  
240 dimensionalities (Section 3.3) 3. Parameter sensitivity: Robustness to hyperparameter  
241 choices (Section 3.4) 4. Feature correlation robustness: Performance under varying levels  
242 of feature correlation (Section 3.5) 5. Pre-filtering value: Benefit of conservative feature  
243 pre-filtering (Section 3.6) 6. Real data validation: Comparative performance against  
244 standard distance metrics on Atlas1006, DietSwap, and SKIOME datasets (Section 3.7) 7.  
245 Biological interpretability: Feature importance weights and visualization (Section 3.8) 8.  
246 Computational performance: Runtime characteristics on standard hardware (Section 3.9)

### 247 *Synthetic data generation*

248 Synthetic datasets were generated using negative binomial count distributions to mimic  
249 microbiome abundance profiles. For each experiment we drew counts as  $X_{ij} \sim NB(\mu =$   
250  $30, size = 0.8)$  and set values smaller than three to zero to induce sparsity. Unless  
251 otherwise noted, we simulated  $n = 100$  samples and  $p = 200$  taxa split evenly across two  
252 groups. To introduce signal we multiplied a subset of taxa in the first group by fold changes  
253 of 1.5 (5 taxa, “small” effect), 2.0 (10 taxa, “medium” effect), or 3.0 (20 taxa, “large” effect).  
254 Sample size ( $n$ ) and dimensionality ( $p$ ) were varied in the scalability experiments (Section  
255 3.3), while null datasets were formed by random label permutations or by shuffling labels  
256 in real data without adding signal.

### 257 *Real data sources*

258 Real microbiome datasets included:

- 259 1. **Atlas1006** (22): 1,114 Western European adults with 123 genus-level taxa from  
260 HITChip microarray technology. Analysis compared males (n=560) versus females  
261 (n=554).
- 262 2. **DietSwap** (23): 74 stool samples from African American adults participating in a  
263 short-term dietary intervention. We analyzed the timepoint-within-group baseline  
264 samples (timepoint.within.group = 1) comparing the Western diet group (HE, n=37)  
265 to the traditional high-fiber diet group (DI, n=37).
- 266 3. **SKIOME** (PRJNA554499): 511 skin microbiome samples across three groups (Atopic  
267 Dermatitis, Healthy, Psoriasis) with 1,856 taxa, used for multi-group validation  
268 across a different body site.

269 Data were preprocessed using centered log-ratio (CLR) transformation for Euclidean  
270 distance analyses to address compositionality (24, 11). CLR transformation converts  
271 relative abundances to log-ratios, making the data suitable for Euclidean distance while  
272 preserving relative relationships between taxa. CLR treats abundance ratios more  
273 equitably than count-based metrics, which can be dominated by highly abundant taxa.  
274 However, CLR transformation may attenuate large fold-change signals compared to count-  
275 based metrics (Bray-Curtis, UniFrac), as evidenced by our results showing that traditional  
276 count-based methods achieve higher F-statistics on synthetic data with large effects ( $3\times$   
277 fold change). CLR is particularly appropriate when signals are distributed across multiple  
278 taxa rather than concentrated in highly abundant taxa, and when interpretability through  
279 feature weights is prioritized. Bray-Curtis dissimilarity, Jaccard, and UniFrac distances  
280 were computed on raw count data, as these metrics are inherently designed to handle  
281 compositional data (25, 7). Prevalence filtering (retaining features present in  $\geq 10\%$  of  
282 samples) is an optional preprocessing step distinct from MeLSI's variance-based pre-  
283 filtering; when applied, prevalence filtering removes rare taxa before analysis, while  
284 MeLSI's pre-filtering focuses on variance-based feature selection after preprocessing.

285 MeLSI was run with 200 permutations to balance computational efficiency with statistical  
286 precision, while traditional PERMANOVA methods used 999 permutations (the field  
287 standard). This conservative comparison favors traditional methods with more precise p-  
288 value estimation, making our results a stringent test of MeLSI's performance.

#### 289 *Comparison methods*

290 MeLSI was compared against standard PERMANOVA analyses using five fixed distance  
291 metrics:

- 292 1. **Euclidean distance:** Standard Euclidean distance calculated on CLR-transformed  
293 data, treating all features equally
- 294 2. **Bray-Curtis dissimilarity:** Count-based dissimilarity metric that accounts for  
295 relative abundances
- 296 3. **Jaccard dissimilarity:** Binary (presence/absence) dissimilarity metric
- 297 4. **Weighted UniFrac:** Phylogenetically-informed distance metric using abundance-  
298 weighted branch lengths (requires phylogenetic tree)
- 299 5. **Unweighted UniFrac:** Phylogenetically-informed distance metric using  
300 presence/absence of taxa along phylogenetic branches (requires phylogenetic tree)

301 To ensure a robust comparison, traditional methods (Weighted/Unweighted UniFrac) were  
302 provided with appropriate phylogenetic structures: random trees for synthetic benchmarks  
303 and published phylogenies for real-world datasets.

#### 304 *Multi-group extensions*

305 For studies with three or more groups, MeLSI provides an omnibus test that jointly  
306 evaluates differences across all groups, with post-hoc pairwise comparisons when  
307 significant. P-values are adjusted for multiple testing using the Benjamini-Hochberg false

308 discovery rate (FDR) procedure (26). The statistical framework (permutation testing, Type I  
309 error control) is identical to two-group analyses, ensuring valid inference regardless of  
310 group number. Real-world validation on the SKIOME skin microbiome dataset (3 groups,  
311 511 samples) demonstrates utility beyond two-group comparisons (see Results section).

## 312 Implementation and computational considerations

313 MeLSI is implemented in R (version >= 4.0) as an open-source package. Key dependencies  
314 include vegan (27) for PERMANOVA calculations, ggplot2 (28) for visualization, and base R  
315 for matrix operations. The algorithm is parallelizable across permutations and weak  
316 learners, though the current implementation is serial.

317 Time complexity is  $O(n^2 p^2 B \cdot n_{\text{perms}})$  in the worst case, but conservative pre-filtering  
318 reduces effective dimensionality, and early stopping in gradient descent reduces iteration  
319 counts. For typical microbiome datasets ( $n < 500$ ,  $p < 1000$ ), analysis completes in minutes  
320 on standard hardware.

## 321 DATA AVAILABILITY

322 MeLSI source code and all validation scripts are permanently archived at Zenodo (DOI:  
323 10.5281/zenodo.17714848) and available at <https://github.com/NathanBresette/MeLSI>  
324 under the MIT license. All validation data and analysis scripts are included in the package  
325 repository for full reproducibility. The Atlas1006 and DietSwap datasets are available  
326 through the R microbiome package (<https://microbiome.github.io/>).

## 327 RESULTS

328 Our validation strategy follows a rigorous progression from statistical validity to biological  
329 utility. We first establish proper Type I error control on null data where no true differences  
330 exist, ensuring MeLSI does not produce false positives despite its adaptive nature. We then  
331 assess statistical power across synthetic datasets with varying effect sizes, comparing  
332 MeLSI's ability to detect true differences against traditional fixed metrics. Finally, we  
333 demonstrate practical utility on real microbiome datasets and evaluate computational  
334 performance, parameter sensitivity, and biological interpretability. This order ensures that  
335 before claiming any advantage, we verify that MeLSI maintains the statistical rigor required  
336 for valid scientific inference.

### 337 Type I error control

338 Proper Type I error control is essential for valid statistical inference. We evaluated MeLSI  
339 on two null datasets where no true group differences exist (Table 1). The first uses  
340 synthetic data with randomly assigned group labels, while the second uses real Atlas1006  
341 data with shuffled group labels (preserving the data structure while breaking group  
342 associations).

### 343 Table 1. Type I Error Control on Null Data

Dataset Type	n	MeLSI Type I	Euclidean Type I	Bray-Curtis Type I	Jaccard Type I	Weighted UniFrac Type I	Unweighted UniFrac Type I
Null Synthetic	50	5%	7%	7%	6%	3%	4%
Null Synthetic	100	4%	3%	2%	5%	2%	4%
Null Synthetic	200	3%	0%	5%	2%	2%	4%
Null Real Shuffled	50	3%	4%	4%	6%	6%	9%
Null Real Shuffled	100	4%	4%	4%	3%	4%	4%
Null Real Shuffled	200	6%	4%	4%	2%	4%	1%

344 Abbreviations: n, sample size; Type I, empirical Type I error rate (percentage of simulations  
 345 with  $p < 0.05$ ). Results based on 100 simulations per condition.

346 Across all conditions, MeLSI maintained proper Type I error control, with empirical  
 347 rejection rates near the nominal 5% level (range: 3-6%). All traditional methods also  
 348 maintained appropriate error rates (range: 0-9%). The permutation testing framework  
 349 properly accounts for the flexibility of learned metrics, ensuring that MeLSI's adaptive  
 350 approach does not inflate false positive rates.

### 351 Performance across synthetic and real datasets

352 We evaluated MeLSI's ability to detect true group differences across synthetic datasets  
 353 with varying effect sizes and real microbiome datasets (Table 2).

354 **Table 2. Statistical Power Analysis Across Effect Sizes and Sample Sizes**

Effect Size	n	MeLSI Power	MeLSI Mean F	MeLSI Rank
Small	50	6%	1.230	1/6
Small	100	10%	1.342	1/6
Small	200	16%	1.432	1/6
Medium	50	16%	1.307	3/6
Medium	100	50%	1.504	3/6
Medium	200	96%	1.780	3/6
Large	50	84%	1.585	3/6
Large	100	100%	2.129	3/6
Large	200	100%	3.129	3/6

355 Abbreviations: n, sample size; Power, empirical statistical power (percentage of  
356 simulations with  $p < 0.05$ ); F, PERMANOVA F-statistic (mean across 50 simulations per  
357 condition); Rank, MeLSI's rank among 6 methods (1/6 = best, 6/6 = worst) based on F-  
358 statistic. Results based on 50 simulations per condition. See Supplementary Tables S1-S2  
359 for recovery metrics and individual method comparisons.

360 MeLSI demonstrated superior sensitivity for subtle signals (small effects, 1.5× fold change),  
361 ranking 1/6 and outperforming all traditional methods. For medium and large effects,  
362 MeLSI achieved competitive performance (3/6 rank) while providing interpretable feature  
363 importance weights. Power increased appropriately with sample size, and learned feature  
364 weights reliably identify true signal taxa (Supplementary Table S1). MeLSI's CLR-based  
365 approach excels at medium effect sizes where signals are distributed across multiple taxa;  
366 for large effects (3× fold change), count-based methods (Bray-Curtis, UniFrac) may be  
367 preferable due to their sensitivity to abundance dominance. The CLR transformation is  
368 most appropriate when signals are distributed across multiple taxa and when  
369 interpretability through feature weights is prioritized.

### 370 Scalability analysis

371 We assessed MeLSI's performance across varying sample sizes (n) and dimensionalities (p)  
372 using synthetic datasets with medium effect sizes (Table 3). For sample size scaling, we  
373 fixed p=200 taxa and varied n from 20 to 500. For dimensionality scaling, we fixed n=100  
374 samples and varied p from 50 to 1000 taxa.

375 **Table 3. Scalability Across Sample Size and Dimensionality**

	n	p	MeLSI F	MeLSI Time	MeLSI Rank
<b>Varying n (p=200)</b>					
n=20	20	200	1.132	486.9	2/6
n=50	50	200	1.277	457.9	2/6
n=100	100	200	1.497	513.3	3/6
n=200	200	200	1.836	739.5	3/6
n=500	500	200	2.511	2055.8	3/6
<b>Varying p (n=100)</b>					
p=50	100	50	1.666	244.8	3/6
p=100	100	100	1.670	337.5	3/6
p=200	100	200	1.470	523.4	3/6
p=500	100	500	1.375	1829.0	1/6
p=1000	100	1000	1.331	8633.0	1/6

376 Abbreviations: n, sample size; p, number of taxa/features; F, PERMANOVA F-statistic; Time,  
377 computation time in seconds; Rank, MeLSI's rank among 6 methods (1/6 = best, 6/6 =

378 worst) based on F-statistic. Values shown as mean across 10 simulations per condition.  
379 See Supplementary Table S3 for individual method comparisons.

380 MeLSI's F-statistics increased monotonically with sample size, demonstrating appropriate  
381 power gains with larger datasets. MeLSI ranked 2/6 at smaller sample sizes and 3/6 at  
382 larger sizes, with computation time scaling as  $O(n^2)$ . Across dimensionalities, MeLSI  
383 ranked 3/6 at lower dimensionalities and 1/6 at higher dimensionalities ( $p \geq 500$ ).  
384 Computation time scales as  $O(p^2)$ , but pre-filtering substantially mitigates this scaling. For  
385 very high-dimensional datasets ( $p > 1000$ ), we recommend pre-filtering, feature aggregation,  
386 or traditional methods if interpretability is not prioritized.

### 387 Parameter sensitivity analysis

388 We evaluated robustness to two key hyperparameters: ensemble size (B) and feature  
389 subsampling fraction (m\_frac) using a synthetic dataset with 100 samples, 200 taxa, and  
390 medium effect size (2 $\times$  fold change in 10 signal taxa) (Table 4).

391 **Table 4. Parameter Sensitivity Analysis**

Parameter	Value	F-statistic	p-value	Time (s)
<b>Ensemble Size (B)</b>				
	1	1.365	0.421	32.9
	10	1.543	0.094	233
	20	1.538	0.089	419.8
	30	1.530	0.091	576.8
	50	1.529	0.093	760
	100	1.528	0.102	1284.1
<b>Feature Fraction (m_frac)</b>				
	0.5	1.578	0.093	405.2
	0.7	1.551	0.083	523.7
	0.8	1.530	0.091	578.2
	0.9	1.517	0.097	630.3
	1.0	1.498	0.100	666.7

392 Abbreviations: B, ensemble size (number of weak learners); m\_frac, feature subsampling  
393 fraction; F, PERMANOVA F-statistic; Time, computation time in seconds. Values shown as  
394 mean across 25 replications per parameter value. See Supplementary Table S4 for  
395 standard deviations.

396 F-statistics remained stable across ensemble sizes (B=10-100), with the single-learner  
397 baseline (B=1) showing substantially higher variance, demonstrating that ensemble  
398 learning reduces variance and prevents overfitting. Performance varied modestly across

399 feature fractions ( $m\_frac=0.5-1.0$ ). The default settings ( $B=30$ ,  $m\_frac=0.8$ ) provide a good  
400 balance between performance and computational cost.

401 **Feature correlation robustness**

402 A critical concern for microbiome data analysis is that taxa are not independent but exhibit  
403 correlations due to ecological relationships (e.g., co-occurring taxa in microbial  
404 communities). To validate MeLSI's robustness to feature correlation, we evaluated  
405 performance across four correlation levels: None ( $r=0$ ), Low ( $r=0.3$ ), Moderate ( $r=0.6$ ), and  
406 High ( $r=0.8$ ), using 50 simulations per condition (200 total simulations) with synthetic  
407 datasets containing 100 samples, 200 taxa, and medium effect size (2 $\times$  fold change in 10  
408 signal taxa) (Table 5).

409 **Table 5. Effect of Feature Correlation on MeLSI Performance**

Correlation Level	Correlation Value	n	MeLSI Power (%)	MeLSI F	Precision at 10	Recall at 10	AUC-ROC	MeLSI Rank
None	0.0	50	50	1.512	0.392	0.392	0.817	3/6
Low	0.3	50	42	1.481	0.348	0.348	0.788	3/6
Moderate	0.6	50	46	1.498	0.356	0.356	0.783	2/6
High	0.8	50	44	1.507	0.368	0.368	0.769	1/6

410 Abbreviations: n, number of simulations per correlation level (not sample size); F,  
411 PERMANOVA F-statistic (mean across 50 simulations); Precision at 10, proportion of top-  
412 10 features that are true signals; Recall at 10, proportion of true signals found in top-10  
413 features; AUC-ROC, area under receiver operating characteristic curve; Rank, MeLSI's rank  
414 among 6 methods (1/6 = best, 6/6 = worst) based on F-statistic. See Supplementary Table  
415 S5 for individual method comparisons.

416 MeLSI demonstrated robust performance across correlation levels, maintaining stable F-  
417 statistics ( $\pm 1.7\%$  variation:  $F=1.512$  at  $r=0$ ,  $F=1.481$  at  $r=0.3$ ,  $F=1.498$  at  $r=0.6$ ,  $F=1.507$  at  
418  $r=0.8$ ) and consistent statistical power (50%, 42%, 46%, 44% respectively). The stability of  
419 F-statistics demonstrates that MeLSI effectively handles correlated features without  
420 performance degradation. Feature recovery metrics also remained stable: Precision at 10  
421 (0.392, 0.348, 0.356, 0.368) and AUC-ROC (0.817, 0.788, 0.783, 0.769) showed minimal  
422 variation across correlation levels, confirming that MeLSI's ability to identify true signal  
423 taxa is maintained even when taxa exhibit high correlation. MeLSI's competitive ranking  
424 (1/6 to 3/6) across all correlation levels demonstrates that the method maintains  
425 statistical power comparable to traditional methods while providing interpretability, even  
426 when features are correlated. Notably, MeLSI achieved its best ranking (1/6) at high  
427 correlation ( $r=0.8$ ), suggesting the method may be particularly effective when taxa exhibit  
428 strong ecological relationships.

429 **Pre-filtering analysis**

430 We evaluated the benefit of conservative pre-filtering by comparing MeLSI with and without  
431 this step using synthetic datasets (n=100 samples per condition) with varying effect sizes  
432 and dimensionalities (small: 1.5× fold change in 5 taxa, p=500; medium: 2.0× in 10 taxa,  
433 p=200; large: 3.0× in 20 taxa, p=100) and high sparsity (70% zero-inflated features) (Table  
434 6).

435 **Table 6. Benefit of Conservative Pre-filtering**

Effect	Features	Filter F	Filter Power	No Filter F	No Filter Power	Delta F	Delta Time
Small	500	1.756	100%	1.281	4%	+37.1 %	+39.8%
Medium	200	1.831	94%	1.337	14%	+36.9 %	+18.0%
Large	100	1.928	84%	1.416	14%	+36.1 %	+16.5%

436 Abbreviations: Effect, effect size category (Small: 1.5× fold change in 5 taxa; Medium: 2.0×  
437 in 10 taxa; Large: 3.0× in 20 taxa); Features, number of taxa; F, PERMANOVA F-statistic  
438 (mean across 50 simulations); Power, empirical statistical power (percentage of  
439 simulations with p < 0.05); Filter, with pre-filtering (top 70% by importance score); No Filter,  
440 without pre-filtering; Delta F, percent change in F-statistic; Delta Time, percent change in  
441 computation time (positive = time savings). Results based on 50 simulations per condition.

442 Variance-based pre-filtering (retaining the top 70% of features by importance score)  
443 demonstrated substantial benefits across all effect sizes. Pre-filtering improved F-  
444 statistics by 36-37% across all effect sizes, increasing power from 4-14% to 84-100% for  
445 small effects. Time savings ranged from 16.5% to 39.8%, increasing with dimensionality.

446 The variance-based importance score ( $I_j = |\mu_{1j} - \mu_{2j}| / \sqrt{\sigma_{1j}^2 + \sigma_{2j}^2}$ ) efficiently identifies  
447 features with large between-group differences relative to within-group variation. Pre-  
448 filtering is particularly valuable when signal is concentrated in a subset of features,  
449 focusing metric learning on the most informative taxa while reducing computational  
450 burden.

451 **Real data validation**

452 To evaluate MeLSI's utility in real-world applications, we analyzed three published  
453 microbiome datasets: Atlas1006 (sex-associated differences), DietSwap (dietary  
454 intervention), and SKIOME (multi-group skin microbiome validation).

455 *Atlas1006 dataset*

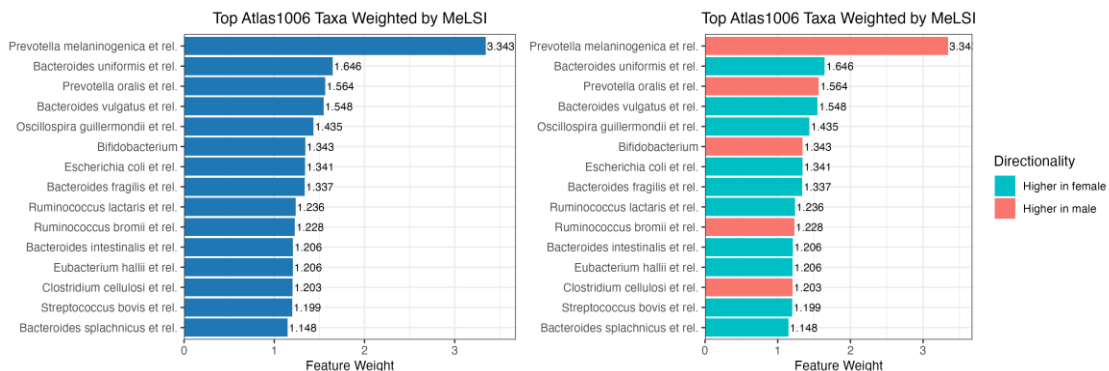
456 On the Atlas1006 dataset (1,114 Western European adults, male vs. female), MeLSI  
457 achieved  $F = 5.141$  ( $p = 0.005$ ) versus  $F = 4.711$  ( $p = 0.001$ ) for Euclidean distance (the best  
458 traditional method), representing a 9.1% improvement. MeLSI's improvement over the best  
459 fixed metric suggests that learned metrics can capture biologically relevant patterns in  
460 subtle, high-dimensional comparisons, consistent with previously documented sex-  
461 associated microbiome differences (29, 30).

462 *DietSwap dataset*

463 On the DietSwap dataset (Western vs. high-fiber diets), MeLSI detected a significant  
464 community difference with  $F = 2.856$  ( $p = 0.015$ ), outperforming all traditional metrics. The  
465 strongest fixed metric was Bray-Curtis ( $F = 2.153$ ,  $p = 0.058$ ). These results suggest that  
466 MeLSI's adaptive weighting captures diet-induced compositional shifts that fixed metrics  
467 only weakly detect.

## 468 Feature importance and biological interpretability

469 MeLSI provides interpretable feature importance weights. For the Atlas1006 dataset, the  
470 learned metric assigned highest weights to genera in the families Bacteroidaceae,  
471 Lachnospiraceae, and Ruminococcaceae, taxonomic groups previously associated with  
472 sex differences in gut microbiome composition (30, 31). Figure 1 displays the top 15 taxa  
473 by learned feature weight.



474

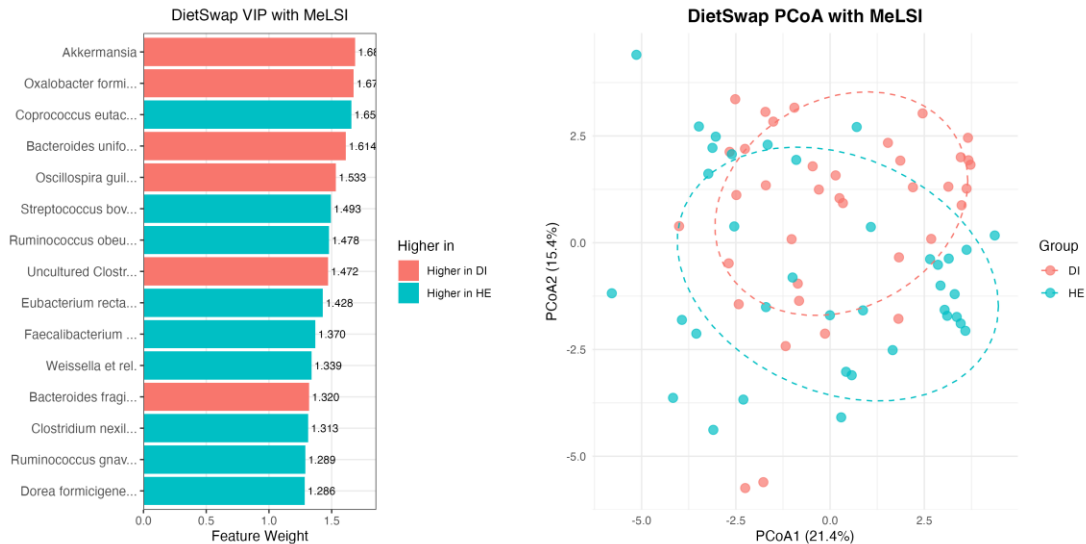
475 **Figure 1.** Top 15 taxa ranked by MeLSI feature weights for Atlas1006 dataset. Left panel  
476 shows feature weights without directionality coloring; right panel shows the same weights  
477 colored by directionality (which group has higher mean CLR abundance). Taxa from  
478 Bacteroidaceae, Lachnospiraceae, and Ruminococcaceae families show strongest  
479 contributions.

480 The diagonal elements of the learned metric matrix  $\mathbf{M}$  directly represent feature  
481 importance: higher values indicate taxa that contribute more to group separation. MeLSI  
482 automatically calculates directionality and effect sizes on CLR-transformed data.  
483 Directionality is determined by identifying which group has the higher mean abundance on  
484 CLR-transformed data, ensuring consistency with the metric learning process. Effect size

485 is reported as the log<sub>2</sub> fold change computed from CLR-transformed group means:  
 486  $\log_2(\mu_{CLR,1}/\mu_{CLR,2})$ . This provides a standardized measure of the magnitude of difference  
 487 between groups for each taxon. The learned distance matrices can also be used for  
 488 Principal Coordinates Analysis (PCoA) ordination to visualize group separation, just as  
 489 traditional distance metrics (Bray-Curtis, Euclidean, etc.) are used with PCoA throughout  
 490 the microbiome field. For datasets where group separation is visually apparent, PCoA  
 491 ordination provides complementary visualization alongside feature importance weights  
 492 (see Figures 2-3 for DietSwap and SKIOME examples).

#### 493 *DietSwap dataset*

494 For the DietSwap dataset, MeLSI's learned feature weights identified taxa including  
 495 Akkermansia and Oxalobacter as key drivers of diet-induced community differences.  
 496 Figure 2 displays the top 15 taxa by learned feature weight alongside the PCoA ordination.

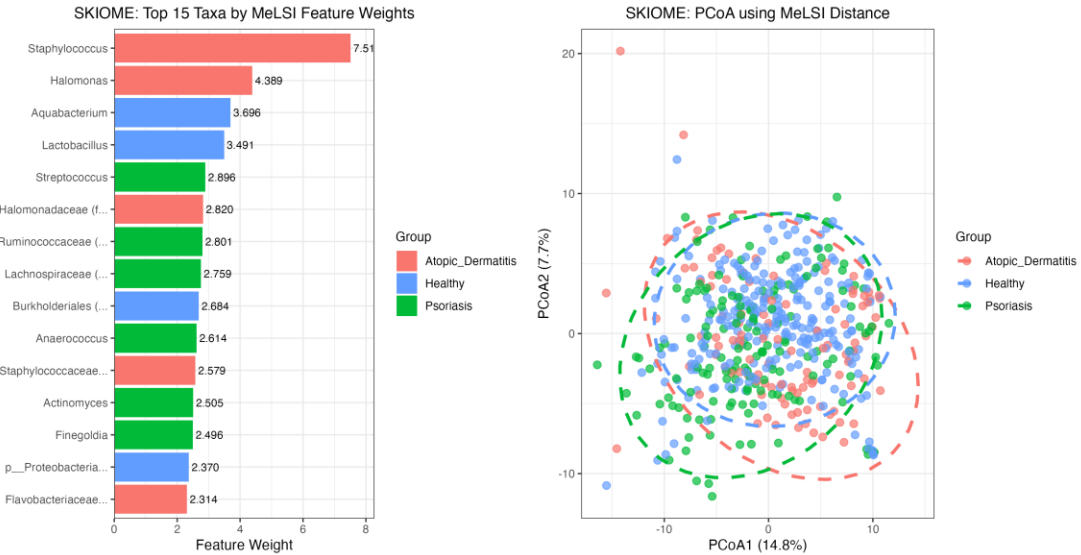


497

498 **Figure 2.** DietSwap dataset: Top 15 taxa by feature weights (left) and PCoA ordination  
 499 (right). Taxa including Akkermansia and Oxalobacter show strong contributions. Dashed  
 500 ellipses show 95% confidence ellipses.

#### 501 *SKIOME dataset: Multi-group validation*

502 To validate multi-group capability, we analyzed the SKIOME skin microbiome dataset  
 503 (PRJNA554499, 511 samples, 3 groups: Atopic\_Dermatitis, Healthy, Psoriasis). MeLSI's  
 504 omnibus test detected significant differences ( $F = 4.895, p = 0.005$ ), comparable to  
 505 Euclidean distance ( $F = 4.897, p = 0.001$ ) but lower than count-based methods (Bray-Curtis:  
 506  $F = 16.275$ , Jaccard:  $F = 11.058$ , both  $p = 0.001$ ). All pairwise comparisons remained  
 507 significant after FDR correction ( $p = 0.005$  for all pairs). Figure 3 displays feature  
 508 importance weights and PCoA ordination, demonstrating MeLSI's interpretability for multi-  
 509 group analyses. This validates MeLSI's utility beyond two-group comparisons and across  
 510 different body sites (skin vs. gut microbiome).



511  
512 **Figure 3.** SKIOME multi-group validation: Feature importance weights (left) and PCoA  
513 ordination (right) for three-group comparison (Atopic\_Dermatitis, Healthy, Psoriasis). Top  
514 15 taxa are colored by the group with highest mean abundance. Dashed ellipses show 95%  
515 confidence ellipses. Consistent with significant omnibus PERMANOVA result ( $F=4.895$ ,  
516  $p=0.005$ ).

517 **Computational performance**

518 Across all experiments, MeLSI demonstrated practical computational performance on  
519 standard hardware. Small datasets ( $n<100$ ,  $p<200$ ) completed in under 2 minutes, medium  
520 datasets ( $n=100-500$ ,  $p=200-500$ ) required 2-15 minutes, and large datasets ( $n=1000+$ ,  
521  $p=100-500$ ) took 15-60 minutes. For comparison, traditional PERMANOVA with fixed  
522 metrics typically completes in under 1 second for similar datasets. However, MeLSI's  
523 additional computation time is justified by improved statistical power and interpretability,  
524 particularly for challenging datasets where fixed metrics perform poorly. Pre-filtering  
525 increases statistical power by 36-37% while reducing computation time by 16-40% (Table  
526 6). For typical microbiome studies ( $n=50-200$ ,  $p=100-500$ ), MeLSI completes in 2-30  
527 minutes (Table 3), representing a modest time investment that yields both improved power  
528 and interpretability through feature weights. For very large studies ( $n>500$ ) or when only  
529 rapid screening is needed, traditional methods may be preferable.

530 **CONCLUSIONS**

531 **Summary**

532 MeLSI bridges adaptive machine learning and rigorous statistical inference for microbiome  
533 beta diversity analysis by integrating metric learning with permutation testing.  
534 Comprehensive validation demonstrates proper Type I error control across 100  
535 simulations per condition, with empirical rejection rates near the nominal 5% level (3-6%  
536 across all conditions and sample sizes) while delivering improvements on real data: 9.1%

537 higher F-statistics on Atlas1006 and significant detection on DietSwap where traditional  
538 metrics remained marginal ( $p = 0.015$  vs.  $p >= 0.058$ ). However, on synthetic datasets with  
539 large effect sizes, count-based (Bray-Curtis) and phylogenetic (UniFrac) methods  
540 demonstrated superior sensitivity, suggesting MeLSI's CLR-transformed approach may not  
541 capture large fold-change signals as effectively as raw count-based metrics.

542 MeLSI's key innovation is interpretability: learned feature weights identify biologically  
543 relevant taxa (e.g., Bacteroidaceae, Lachnospiraceae, Ruminococcaceae in sex-  
544 associated differences), turning omnibus PERMANOVA results into actionable biological  
545 insights. MeLSI is recommended when: (1) effect sizes are moderate (2 $\times$  fold change)  
546 rather than very large, (2) interpretability through feature weights is needed to identify  
547 biologically relevant taxa, (3) traditional methods yield marginal results (p-values near  
548 0.05), and (4) signals are distributed across multiple taxa rather than concentrated in  
549 highly abundant taxa. Traditional methods (Bray-Curtis, UniFrac) are preferable for: (1)  
550 large, obvious effects (3 $\times$  fold change) where any method succeeds, (2) large-scale  
551 screening studies where speed is critical, and (3) when only omnibus significance testing is  
552 needed without feature-level interpretation. Critically, unlike prediction-focused machine  
553 learning (e.g., Random Forest, neural networks), MeLSI is an inference-focused approach:  
554 every learned metric undergoes rigorous permutation testing to ensure that p-values  
555 remain valid despite the adaptive nature of the method. This distinction is fundamental:  
556 MeLSI prioritizes statistical rigor over predictive accuracy, maintaining Type I error control  
557 while adapting to dataset-specific signal structure.

## 558 Limitations and future work

559 MeLSI requires more computation time than fixed metrics (minutes vs. seconds), reflecting  
560 the cost of learning optimal metrics through ensemble training and permutation testing.  
561 However, MeLSI's computational time (2-30 minutes for typical datasets) is justified by  
562 substantial interpretability gains through learned feature weights, combined with a  
563 favorable power-time trade-off through pre-filtering (Table 6). For large-scale screening  
564 studies with thousands of samples, traditional methods may be more appropriate.

565 Synthetic validation focused on two-group comparisons, which represent the primary use  
566 case; multi-group synthetic validation would require duplicating all validation tables and is  
567 addressed through real-world multi-group validation on the SKIOME skin microbiome  
568 dataset (3 groups, 511 samples). The statistical framework (permutation testing, Type I  
569 error control) is identical for two-group and multi-group analyses, ensuring valid inference  
570 regardless of group number.

571 The most immediate extensions are (1) regression and covariate adjustment to handle  
572 continuous outcomes and confounders (age, BMI, medication use), enabling integration  
573 with epidemiological frameworks, (2) paired and longitudinal design support through  
574 blocked permutations (restricting permutations within subjects or pairs via the strata  
575 argument in PERMANOVA), and (3) improved compositionality handling by learning metrics

576 directly in compositional space using Aitchison geometry (24), potentially offering  
577 advantages for zero-inflated microbiome data.

578 MeLSI's learned distance metrics are compatible with other distance-based ordination  
579 and hypothesis testing methods. The learned distances can be used with Non-metric  
580 Multidimensional Scaling (NMDS) (32) and Analysis of Similarities (ANOSIM) (33), both of  
581 which operate on distance matrices and would benefit from MeLSI's data-adaptive metrics.  
582 However, Principal Component Analysis (PCA) is not compatible with MeLSI's learned  
583 distances, as PCA relies on Euclidean distances computed in the original feature space  
584 and cannot accommodate the learned Mahalanobis distance structure.

## 585 Software availability

586 MeLSI is freely available as an open-source R package under the MIT license at  
587 <https://github.com/NathanBresette/MeLSI> (DOI: 10.5281/zenodo.17714848). The package  
588 is currently under review for inclusion in Bioconductor. The package includes  
589 comprehensive documentation, tutorial vignettes, and example datasets. All validation  
590 experiments are fully reproducible using provided code and data. Recommended usage:  
591 aim for  $n \geq 50$  per group, apply CLR transformation, use default settings ( $B=30$ ,  
592  $m_{frac}=0.8$ ,  $n_{perms}=200$ ), and validate top-weighted features with univariate differential  
593 abundance methods.

## 594 SUPPLEMENTARY MATERIAL

595 Supplementary tables providing detailed results are available:

- 596 • **Supplementary Table S1:** Recovery of true signal taxa metrics (Precision at k,  
597 Recall at k, Mean Rank, AUC-ROC) across all effect sizes and sample sizes
- 598 • **Supplementary Table S2:** Individual method comparisons for power analysis  
599 (MeLSI vs. each traditional method) supporting rank calculations in Table 2
- 600 • **Supplementary Table S3:** Individual method comparisons for scalability analysis  
601 supporting rank calculations in Table 3
- 602 • **Supplementary Table S4:** Parameter sensitivity analysis with standard deviations  
603 (mean and SD for F-statistics, p-values, and computation times across 25  
604 replications per parameter value)
- 605 • **Supplementary Table S5:** Individual method comparisons for feature correlation  
606 analysis

607 These supplementary tables provide complete transparency for rank calculations (e.g., 1/6,  
608 3/6) shown in the main tables, allowing readers to see how MeLSI compares to each  
609 traditional method individually.

## 610 FUNDING

611 This work was supported by the National Institutes of Health/National Institute on Aging  
612 (NIH/NIA) grant R56AG079586 to A-LL.

613 **ACKNOWLEDGMENTS**

614 Computational resources were provided by the University of Missouri Research Computing  
615 (Hellbender HPC cluster). We acknowledge the use of Hellbender computational  
616 resources (DOI: 10.32469/10355/97710).

617 **AUTHOR CONTRIBUTIONS**

618 Nathan Bresette conceived the study, developed the methodology, implemented the  
619 software, performed all analyses, generated all figures and tables, and wrote the  
620 manuscript. Aaron C. Ericsson provided substantial guidance on methodological  
621 development and improvements to the method and interpretability. Carter Woods  
622 contributed ideas and assisted with manuscript editing. Ai-Ling Lin provided project  
623 leadership and oversight as principal investigator.

624 **COMPETING INTERESTS**

625 The authors declare no competing interests.

626 **ORCID**

627 Nathan Bresette: <https://orcid.org/0009-0003-1554-6006>

628 Aaron C. Ericsson: <https://orcid.org/0000-0002-3053-7269>

629 Carter Woods: <https://orcid.org/0009-0007-5345-2712>

630 Ai-Ling Lin: <https://orcid.org/0000-0002-5197-2219>

631 **AUTHOR AFFILIATIONS**

632 <sup>1</sup> Roy Blunt NextGen Precision Health, University of Missouri, Columbia, Missouri, USA.

633 <sup>2</sup> Institute for Data Science and Informatics, University of Missouri, Columbia, Missouri,  
634 USA.

635 <sup>3</sup> Bioinformatics and Analytics Core, University of Missouri, Columbia, Missouri, USA.

636 <sup>4</sup> Department of Pathobiology and Integrative Biomedical Sciences, University of Missouri,  
637 Columbia, Missouri, USA.

638 <sup>5</sup> Department of Radiology, University of Missouri, Columbia, Missouri, USA.

639 <sup>6</sup> Division of Biological Sciences, University of Missouri, Columbia, Missouri, USA.

640 **REFERENCES**

- 641 1. Gilbert JA, Blaser MJ, Caporaso JG, Jansson JK, Lynch SV, Knight R. 2018. Current  
642 understanding of the human microbiome. Nat Med 24:392-400.

- 643 2. Shreiner AB, Kao JY, Young VB. 2015. The gut microbiome in health and in disease.  
644 Curr Opin Gastroenterol 31:69-75.

645 3. Lynch SV, Pedersen O. 2016. The human intestinal microbiome in health and  
646 disease. N Engl J Med 375:2369-2379.

647 4. Clemente JC, Ursell LK, Parfrey LW, Knight R. 2012. The impact of the gut  
648 microbiota on human health: an integrative view. Cell 148:1258-1270.

649 5. Anderson MJ. 2017. Permutational multivariate analysis of variance (PERMANOVA),  
650 p 1-15. In Wiley StatsRef: Statistics Reference Online. John Wiley & Sons, Ltd.

651 6. McArdle BH, Anderson MJ. 2001. Fitting multivariate models to community data: a  
652 comment on distance-based redundancy analysis. Ecology 82:290-297.

653 7. Lozupone C, Knight R. 2005. UniFrac: a new phylogenetic method for comparing  
654 microbial communities. Appl Environ Microbiol 71:8228-8235.

655 8. Ramette A. 2007. Multivariate analyses in microbial ecology. FEMS Microbiol Ecol  
656 62:142-160.

657 9. Knights D, Costello EK, Knight R. 2011. Supervised classification of human  
658 microbiota. FEMS Microbiol Rev 35:343-359.

659 10. Weiss S, Xu ZZ, Peddada S, Amir A, Bittinger K, Gonzalez A, Lozupone C, Zaneveld JR,  
660 Vázquez-Baeza Y, Birmingham A, Hyde ER, Knight R. 2017. Normalization and  
661 microbial differential abundance strategies depend upon data characteristics.  
662 Microbiome 5:27.

663 11. Gloor GB, Macklaim JM, Fernandes AD. 2017. Displaying variation in large datasets:  
664 plotting a visual summary of effect sizes. J Comput Graph Stat 25:971-979.

665 12. Westfall PH, Young SS. 1993. Resampling-Based Multiple Testing: Examples and  
666 Methods for p-Value Adjustment. John Wiley & Sons, New York, NY.

667 13. Good PI. 2013. Permutation Tests: A Practical Guide to Resampling Methods for  
668 Testing Hypotheses. Springer Science & Business Media, New York, NY.

669 14. Kulis B. 2013. Metric learning: a survey. Found Trends Mach Learn 5:287-364.

670 15. Bellet A, Habrard A, Sebban M. 2013. A survey on metric learning for feature vectors  
671 and structured data. arXiv:1306.6709.

672 16. Weinberger KQ, Saul LK. 2009. Distance metric learning for large margin nearest  
673 neighbor classification. J Mach Learn Res 10:207-244.

- 674        17. Xing EP, Jordan MI, Russell SJ, Ng AY. 2002. Distance metric learning with  
675              application to clustering with side-information, p 521-528. In Advances in Neural  
676              Information Processing Systems 15.
- 677        18. Mahalanobis PC. 1936. On the generalized distance in statistics. Proc Natl Inst Sci  
678              India 2:49-55.
- 679        19. Pasolli E, Truong DT, Malik F, Waldron L, Segata N. 2016. Machine learning meta-  
680              analysis of large metagenomic datasets: tools and biological insights. PLoS Comput  
681              Biol 12:e1004977.
- 682        20. Breiman L. 2001. Random forests. Mach Learn 45:5-32.
- 683        21. Phipson B, Smyth GK. 2010. Permutation p-values should never be zero: calculating  
684              exact p-values when permutations are randomly drawn. Stat Appl Genet Mol Biol  
685              9:Article39.
- 686        22. Lahti L, Salojärvi J, Salonen A, Scheffer M, de Vos WM. 2014. Tipping elements in the  
687              human intestinal ecosystem. Nat Commun 5:1-10.
- 688        23. O'Keefe SJD, Li JV, Lahti L, Ou J, Carbonero F, Mohammed K, Posma JM, Kinross J,  
689              Wahl E, Ruder E, Vipperla K, Naidoo V, Mtshali L, Tims S, Puylaert PGB, DeLany J,  
690              Krasinskas A, Benefiel AC, Kaseb HO, Newton K, Nicholson JK, de Vos WM, Gaskins  
691              HR, Zoetendal EG. 2015. Fat, fibre and cancer risk in African Americans and rural  
692              Africans. Nat Commun 6:6342.
- 693        24. Aitchison J. 1986. The Statistical Analysis of Compositional Data. Chapman and  
694              Hall, London.
- 695        25. Legendre P, Gallagher ED. 2001. Ecologically meaningful transformations for  
696              ordination of species data. Oecologia 129:271-280.
- 697        26. Benjamini Y, Hochberg Y. 1995. Controlling the false discovery rate: a practical and  
698              powerful approach to multiple testing. J R Stat Soc Series B Stat Methodol 57:289-  
699              300.
- 700        27. Oksanen J, Blanchet FG, Friendly M, Kindt R, Legendre P, McGlinn D, Minchin PR,  
701              O'Hara RB, Simpson GL, Solymos P, Stevens MHH, Szoecs E, Wagner H. 2020.  
702              vegan: Community Ecology Package. R package version 2.5-7. <https://CRAN.R-project.org/package=vegan>.
- 704        28. Wickham H. 2016. ggplot2: Elegant Graphics for Data Analysis. Springer-Verlag,  
705              New York, NY.
- 706        29. Markle JGM, Frank DN, Mortin-Toth S, Robertson CE, Feazel LM, Rolle-Kampczyk U,  
707              von Bergen M, McCoy KD, Macpherson AJ, Danska JS. 2013. Sex differences in the  
708              gut microbiome drive hormone-dependent regulation of autoimmunity. Science  
709              339:1084-1088.

- 710        30. Org E, Mehrabian M, Parks BW, Shipkova P, Liu X, Drake TA, Lusis AJ. 2016. Sex  
711        differences and hormonal effects on gut microbiota composition in mice. *Gut*  
712        *Microbes* 7:313-322.
- 713        31. Vemuri R, Gundamaraju R, Shastri MD, Shukla SD, Kalpurath K, Ball M, Tristram S,  
714        Shankar EM, Ahuja K, Eri R. 2019. Gut microbial changes, interactions, and their  
715        implications on human lifecycle: an ageing perspective. *Biomed Res Int*  
716        2019:4178607.
- 717        32. Kruskal JB. 1964. Nonmetric multidimensional scaling: a numerical method.  
718        *Psychometrika* 29:115-129.
- 719        33. Clarke KR. 1993. Non-parametric multivariate analyses of changes in community  
720        structure. *Aust J Ecol* 18:117-143.